CRYSTAL GROWTH & DESIGN

Article

Hydrothermal Crystal Growth of Mixed Valence CsSbBr

Victoria E. Combs, Iain W. H. Oswald, and James R. Neilson

Cryst. Growth Des., **Just Accepted Manuscript** • Publication Date (Web): 22 May 2019

Hydrothermal Crystal Growth of Mixed Valence Cs_2SbBr_6

Victoria E. Combs, Iain W. H. Oswald, and James R. Neilson*

Department of Chemistry, Colorado State University, Fort Collins, CO, 80523-1872

E-mail: james.neilson@colostate.edu

Abstract

Mixed valence perovskite materials present an opportunity to understand how structural motifs influence electronic properties in semiconducting materials. Here, we report the preparation of high-quality single crystals of the mixed valence compound Cs_2SbBr_6, which can also be written as $Cs_4Sb^{III}Sb^{V}Br_{12}$. We have determined the solubility of Cs_2SbBr_6 under myriad reaction conditions which permits prescription of conditions to grow large, high-quality single crystals. Single crystal X-ray diffraction confirms the crystal structure of this material and shows that the crystal structure is preserved from T = 100 to 380 K, and the heat capacity measurements show an absence of any anomalies due to phase transitions between T = 2 to 150 K. Furthermore, we illustrate that the mixed valence of the Sb centers in this material charge order into interpenetrating diamond lattices. We also show that the habit of Cs_2SbBr_6 single crystals is defined by well-formed faces along the close packed planes of bromine atoms.

Introduction

Semiconductors incorporating mixed valence ions continue to garner interest due to the variety of fascinating properties that result from the complex electronic structures. The rich magnetic

phase diagram and metal-insulator behavior of manganese oxide perovskites[1] and the superconductivity of bismuth oxide based perovskites[2] are two famous instances in which the emergent electronic ground states result from the incorporation of mixed valence metals. Although the electronic ground states of mixed valence materials have been heavily studied, less is understood about the nature of excited states resulting from mixed valence systems. For example, little is known about the states created from the charge transfer between mixed valence species caused by visible light absorption. The excitement surrounding the high-performance halide semiconductors such as $CH_3NH_3PbI_3$[3] and Cs_2SnI_6[4] encourages renewed interest in, and expansion of, the early studies on antimony-based halides,[5] such as in the vacancy-ordered double perovskite (VODP) Cs_2SbBr_6.[6]

Mixed valence VODP halides can be described by the formula "$A_4B^{III}B^{V}X_{12}$", as the formally tetravalent B site metal charge disproportionates from B^{4+} into B^{5+} and B^{3+} when considering formal charge.[5] In Cs_2SbBr_6, this charge disproportionation is accompanied by distortion from O_h symmetry of the [$SbBr_6$] octahedra to D_{2h} symmetry, where the axial bonds are elongated and the equatorial bonds are shortened.[7] The ordering of $[SbX_6]^-$ and $[SbX_6]^{3-}$ octahedra results in the tetragonal space group $I4_1/amd$. These materials also exhibit visible and near-IR light absorption due to charge transfer from the fully occupied Sb^{3+} 5s orbitals to the unoccupied 5s orbitals of Sb^{5+}.[8,9] The charge transfer processes have also been shown to be intimately coupled to vibrational modes within the material.[10] However, detailed investigations into electronic transport awaits the synthesis of single crystalline specimens of these materials.

Here, we report the hydrothermal preparation of single crystalline mixed valence VODP Cs_2SbBr_6. The solubility behavior of the system has been investigated under many different reaction conditions. The results allow prescription of suitable concentrations which produce large crystal growth at various temperatures, as experimentally verified. The crystal structure of Cs_2SbBr_6 was investigated using single crystal X-ray diffraction (SCXRD) and is consistent with previous reports.

Methods and Materials

Preparation of Cs_2SbBr_6 Powder

Polycrystalline powders of Cs_2SbBr_6 were synthesized via solution precipitation following previous reports.[7] Sb powder (∼0.060 g, NOAH, 99.5%) was added to ∼5 mL aqueous HBr (Sigma-Aldrich, 48%) with stirring, after which ∼100 μL of Br_2 (Alfa Aesar, 99.8%) liquid was pipetted into the mixture. The mixture was then heated to ∼60 °C with magnetic stirring until all Sb powder dissolved. A solution of Cs_2CO_3 (∼0.160 g, Alfa Aesar, 99.9%) dissolved in 3 mL aqueous HBr (to produce a CsBr solution) was then added to the Sb solution with stirring. A fine black precipitate formed upon addition of the CsBr solution and the reaction was stirred for an additional 30 min. The powder was allowed to settle before the supernatant was removed. The powder was then dried in a desiccator that also contained a beaker of concentrated H_2SO_4 (EMD, Millipore, 98%) and a beaker containing ∼100 μL of Br_2 liquid. Cs_2SbBr_6 powder was synthesized up to a purity of 99.1(1) wt% , and powder X-ray diffraction (PXRD) data are consistent with the reported crystal structure.[7] The purity of powder was calculated from Reitveld refinement. The major impurities determined by Rietveld refinement are the cesium and bromine deficient phase $Cs_3Sb_2Br_9$ and CsBr. Allowing the powder to dry in air or under N_2 results in decomposition to the yellow competing phase $Cs_3Sb_2Br_9$ and CsBr.

Hydrothermal Growth

Hydrothermal crystallization was carried out in Parr Instrument Company Model 4749 and 4745 acid digestion vessels (23 mL and 45 mL capacity respectively) in a Binder APT.line FP convection oven. To ensure the vessels were free of contamination prior to crystallization experiments, the autoclaves were treated with ∼8 mL HNO_3 and heated at 150 °C for 24 h. The vessels were subsequently charged with ∼8 mL unpurified H_2O and heated at 150 °C for 24 h to rinse. This rinse was repeated until contents of the vessel were pH neutral. Each autoclave was charged with previously-prepared Cs_2SbBr_6 powder, 2-8 mL HBr, and 4 molar equivalents of Br_2 relative to

Cs_2SbBr_6. The reactions were heated to 150 °C over 1 h and then dwelled at temperature for 5 h before being slowly cooled over 7 days. All crystals were stored in a desiccator that also contained a beaker of concentrated H_2SO_4 and a beaker containing ∼100 μL of Br_2 liquid. To clean the vessels after each reaction the vessels were charged with unpurified H_2O and heated at 150 °C for 24 h.

Solubility Experiments

Between 10 mg to 250 mg of Cs_2SbBr_6 powder were placed in each of 6 autoclaves. 2.0 mL of HBr was added to each autoclave followed by 4 molar equivalents (with respect to powder) of Br_2. The estimated nominal concentrations of Cs_2SbBr_6 ranged from 0.000012-0.28 M. Reaction vessels were heated to 125 °C, 150 °C, and 175 °C and allowed to dwell for 1 h before being cooled to room temperature. The vessels were then opened and inspected for undissolved powder. Solubility behavior was assessed by the presence of undissolved powder or the lack thereof.

Characterization

Laboratory powder X-ray diffraction (PXRD) data were collected on a Bruker D8 Discover X-ray diffractometer using Cu Kα radiation and a Lynxeye XE-T position sensitive detector. All samples were ground in an agate mortar and pestle before being affixed to a "Zero Diffraction" silicon wafer with a small amount of Vaseline®. Quantitative analysis of PXRD data was accomplished by the Rietveld method as implemented in GSAS/EXPGUI[11] (Figure S3).

Single-crystal X-ray diffraction (SCXRD) was performed using a Bruker D8 Quest single crystal X-ray diffractometer with a microfocus Mo Kα radiation source and Photon 50 CMOS half-plate detector. Data collected at $T = 100$ K were from a single crystal mounted on a MiTeGen tip using Paratone® oil. Both $T = 300$ K and $T = 380$ K measurements were performed using a single crystal affixed to a glass fiber with epoxy.

The initial structural model was obtained from the previously reported crystal structure which was further refined using SHELXTL Version 2017/1.[12] Bruker SAINT was used for integration

and scaling of collected data and SADABS was used for absorption correction.[13] VESTA was used to render all crystal structures.[14]

Heat capacity measurements were performed on pelleted samples using the quasi-adiabatic heat-pulse technique implemented in the Quantum Design, Inc., PPMS at T = 2-150 K, equilibrating for four time constants. Laue diffraction was performed on a back-reflection Laue diffractometer from Photonic Science and Engineering, Ltd. with a source to sample distance of 46.41 mm.

Results and Discussion

The solubility behavior of Cs_2SbBr_6 was investigated to provide insight into the crystallization process under hydrothermal reaction conditions. The reactions with the highest concentration of powder that fully dissolve at a specific temperature comprise the solubility curve of the system, as shown in Figure 1. From this curve, we estimate the molar solubility at each reaction temperature (Table 1).

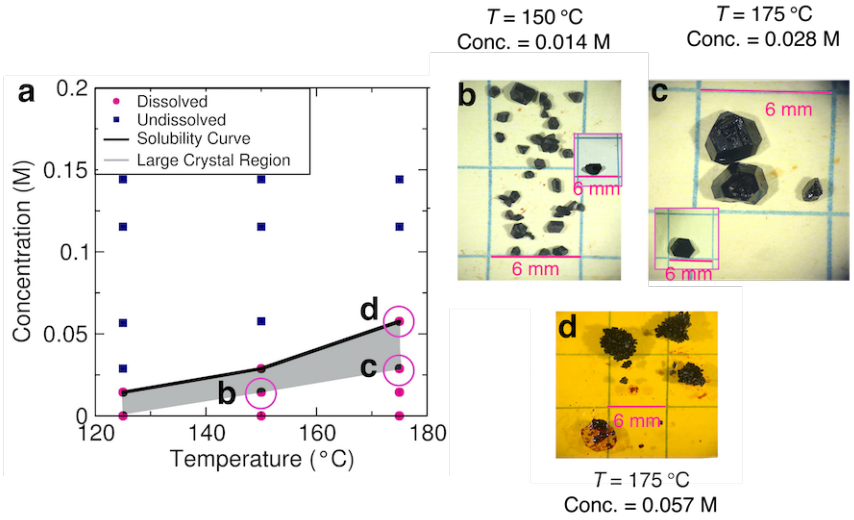

Figure 1: Solubility behavior of Cs_2SbBr_6 during hydrothermal reactions at various temperatures

As the reaction temperature increases, the concentration at which full solubilization of powder occurs also increases. We find that the largest crystals form just below the solubility curve. The largest crystals produced at 125 °C were grown around concentrations of 0.1 M (Fig 1b).

Table 1: Molar solubility of Cs_2SbBr_6 for each hydrothermal crystal growth reaction temperature

Temperature (°C)	Molar Solubility (M)
125	0.01447
150	0.02883
175	0.05767

Preparation of large single crystals also requires sufficient volume of mother liquor. Crystal growth experiments in volumes ranging from 1 mL to 8 mL while concentration was constant suggest that larger, higher quality crystals are formed with a higher volume. We hypothesize that this is due to increased convective mixing which occurs in higher volume samples compared to lower volume samples.

Crystal growth experiments performed at 175 °C with a concentration of 0.028 M reproducibly yields 3 to 4 mm on-a-side single crystals(Fig 1c). At concentrations of 0.057 M, agglomerated crystals are produced along with several small single crystals (Fig 1d). This is likely due to the high concentration precluding all powder from dissolving during heating and results in powder-induced nucleation points.

Cs_2SbBr_6 crystallizes in the tetragonal $I4_1/amd$ space group and adopts a VODP structure where each Sb center is octahedrally coordinated to six Br^- with Cs^+ situated at the *A* site. In their report of the crystal structure of Cs_2SbBr_6, Prassides and Day determined that the bond lengths of Sb-Br differ between the Sb^{III} and Sb^{V} sites, making each Sb site crystallographically distinct, suggesting a chemical formula of "$Cs_4Sb^{III}Sb^{V}Br_{12}$".[7] The slight differences in bond length between Sb^{III}-Br and Sb^{V}-Br order crystallographically and cause the cubic unit cell to double along the *c* axis, forming a supercell and an overall tetragonal unit cell. Precession images produced during SCXRD data collection are shown in Figure 3 and feature intense spots corresponding to a nominally cubic cell while the weaker reflections in between are evidence of the superlattice reported in this material.[8]

To determine the crystal structure, Prassides and Day relied on powder neutron diffraction data collected at $T = 4.7$ K. The authors reported several peaks in their diffraction pattern which could not be identified as impurities or the lower symmetry space group $I4_1/a$.[7] SCXRD data was ob-

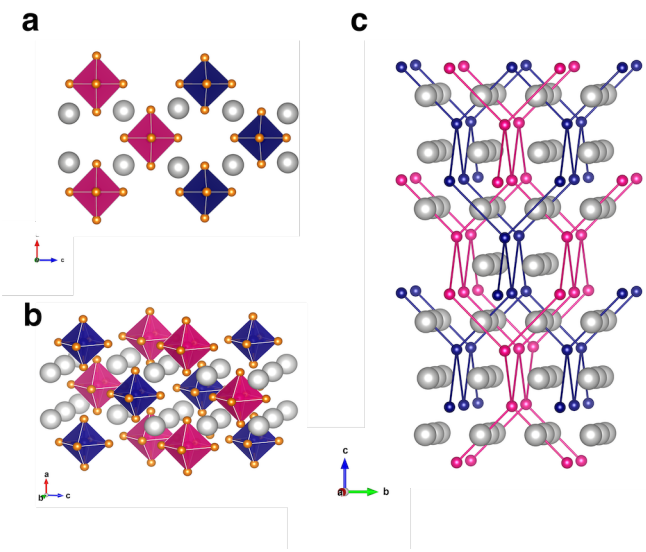

Figure 2: **a** Crystal structure of Cs_2SbBr_6 showing one slice of octahedra and **b** showing the absence of covalent connectivity between octahedra. **c** Lines drawn between like Sb centers to show the interpenetrating diamond lattices created by the charge ordering of Sb centers. Cs is light gray, Sb^{III} is dark blue, Sb^{V} is magenta, and Br is orange. Br has been omitted in **b** for clarity.

tained at 380 K, 300 K, and 100 K to determine if Cs_2SbBr_6 undergoes crystallographic phase transitions that could account for these peaks. The data collected at all three temperatures are consistent with the original structure reported by Prassides and Day, indicating that the crystallographic structure of Cs_2SbBr_6 is preserved between 100 K and 380 K. Furthermore, experimental determination of the specific heat between T = 2-150 K does not reveal any enthalpy-releasing transitions (Fig 4).

Table 2: Comparison of crystal structure determination results from SCXRD data collected at 300 K. and 380 K and original crystal structure determination from powder neutron diffraction data collected at 4.7 K.[7] Further crystallographic details are available in Table S1.

	Crystallographic Data			
Temperature	4.7 K[7]	100K	300 K	380 K
Space Group	$I4_1/amd$	$I4_1/amd$	$I4_1/amd$	$I4_1/amd$
a, Å	10.7320(1)	10.7535(8)	10.842(3)	10.888(3)
c, Å	21.7442(2)	21.6794(16)	21.91(15)	21.979(6)
Avg Sb^{III}–Br Bond Length, Å	2.733(2)	2.7672(7)	2.7842(9)	2.7897(12)
Avg Sb^{V}–Br Bond Length, Å	2.580(5)	2.5736(2)	2.5661(3)	2.5627(12)

Based on these data, Cs_2SbBr_6 appears to undergo positive thermal expansion upon heating

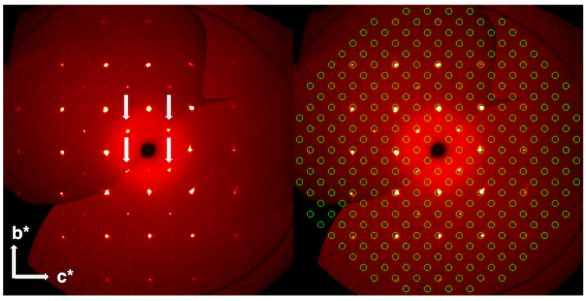

Figure 3: Single crystal XRD precession images collected at 380 K along the (0kl) direction showing clarity and intensity of reflections. The reflections corresponding to the cubic lattice observed for most VODPs are especially intense and those corresponding to the tetragonal superlattice occur in between the more intense cubic reflections.

although the average bond lengths of Sb^{V}-Br contract as temperature increases. Bond length contraction has been reported to stem from continuous charge transfer in $SrCu_3Fe_4O_{12}$ [15] so it is likely that the well-known charge transfer in these materials is responsible for the Sb^{V}-Br bond length contraction. Similar behavior in the $CsSnBr_3$ perovskite has been reported and is likely to manifest due to stereochemically active lone pairs on the Sn center.[16] However in Cs_2SbBr_6, we find no contraction of the Sb^{III}-Br bonds, allowing us to conclude that stereochemically active lone pairs on the Sb^{III} center are unlikely to be the source of the bond length contraction exhibited by Cs_2SbBr_6.

Bond valence sum calculations for the Sb centers were performed to elucidate the valence of each Sb center and to determine the degree of delocalization of charge between metal centers.[17] Calculated bond valences suggest the Sb centers retain oxidation states consistent with localized Sb^{III} and Sb^{V} charges.

Table 3: Bond valence sums calculated from SCXRD data collected at 300 K.

Atom	300 K	R_0	β
Sb^{III}	3.0	2.51	0.37
Sb^{V}	4.7	2.48	0.37

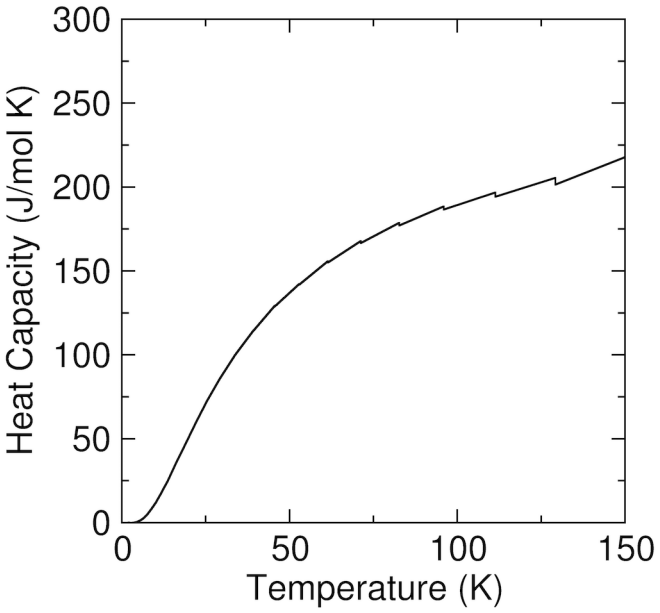

Figure 4: Heat capacity data for Cs_2SbBr_6 showing a lack of phase transitions between T = 2-150 K.

Double perovskites tend to order in a checkerboard pattern in order to minimize the energy from electrostatic interactions.[18] However, this checkerboard motif is not observed in Cs_2SbBr_6. The charge ordering of Sb centers can be described as two interpenetrating diamond lattices of like-valence antimony. Figure 2b shows that Sb^{III} and Sb^{V} centers each form a diamond lattice to create a charge ordering pattern in Cs_2SbBr_6 that resembles Cu_2O elongated along one crystallographic axis.[19]

Cs_2SbBr_6 forms shiny black crystals with a variety of habits and well defined, smooth faces as shown in Figure 1. Usually the habit forms as a truncated octahedron and appears nearly hexagonal. Insight into the crystal habit is provided by performing Laue diffraction on large single crystals. Mounting crystals such that their largest faces are orthogonal to the incident beam, we readily identified the $(00\bar{1})$ zone axes, as illustrated in Figure 5 and Figure S1 . The habit of Cs_2SbBr_6 crystals is rationalized by considering the arrangement of octahedra in the crystal structure of this material. The apparent zero-dimensional connectivity of Cs_2SbBr_6 creates natural cleavages which stabilize crystal face formation as shown in Figure 2c. This formation yields no dangling Sb-Sb bonds and

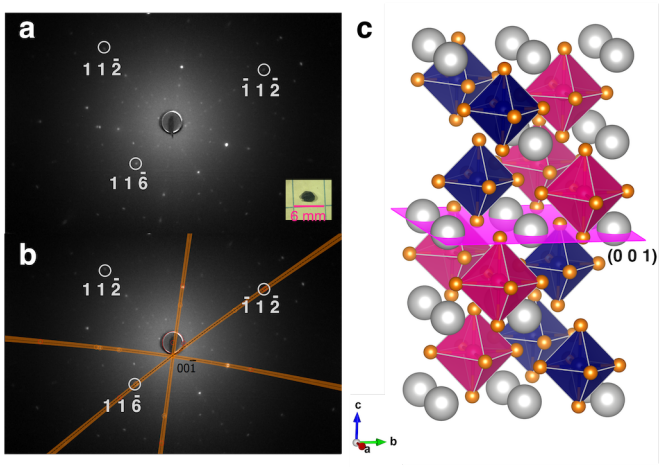

Figure 5: Laue diffraction image showing the **a** $(00\bar{1})$ zone axis and **b** the corresponding fit with selected points indexed. **c** shows the crystal structure of Cs_2SbBr_6 with the $(00\bar{1})$ plane indicated in pink.

can be electrostatically screened by the protic, polar solvent. Further Laue experiments suggest that a large crystal face can also be preferentially formed along the $\{112\}$ planes of Cs_2SbBr_6 as shown in Figure S2. This family of planes cuts through the close-packed sublattice of bromine atoms forming a stable plane for growth of a stable face. These planes were identified by performing Laue diffraction at a perpendicular face and using the stereographic projection to determine the face 90° from the diffracted plane. It is probable that both the $\{112\}$ and $\{001\}$ form comparably stable crystal faces and that individual crystals can form large faces along these planes depending on their habit. The octahedral faces of the crystal habit are thus likely composed of the $\{112\}$ faces, comprised of the close-packed anionic planes.

Conclusions

Hydrothermal reactions in aqueous HBr are used to produce large single crystals of the defect perovskite Cs_2SbBr_6. The solubility behavior of the compound is reported at multiple temperatures. Specific heat measurements from 2-150 K suggest an absence of any phase transitions. When compared with SCXRD, we conclude that the crystal structure of Cs_2SbBr_6 is preserved from T = 2-380 K. Furthermore, examination of the crystal structure shows that the mixed valence Sb

centers in Cs_2SbBr_6 produce a charge ordering pattern in which the Sb centers order into interpenetrating diamond lattices. The habit of single crystalline Cs_2SbBr_6 is defined by large faces along close-packed planes of anions or between octahedra.

Acknowledgments

This work was supported by Grant DE-SC0016083 funded by the U.S. Department of Energy, Office of Science. J.R.N. and V.E.C. acknowledge support from Research Corporation for Science Advancement through a Cottrell Scholar Award, and J.R.N. thanks the A.P. Sloan Foundation for assistance provided from a Sloan Research Fellowship. V.E.C. thanks Dr. A.E. Maughan, D.R. Yahne, and Dr. K.A. Ross for assistance.

Additional Information

Supporting Info

Crystallographic information files (CIFs) Laue diffraction images and fits for (001) and (112) planes Crystallographic details for Cs_2SbBr_6 at 100 K, 300 K, and 380 K. Powder X-ray diffraction of Cs_2SbBr_6

Author Information

Corresponding Author

james.neilson@colostate.edu

Notes

The authors declare no competing financial interest.

References

(1) Coey, J.; Viret, M.; Von Molnar, S. Mixed-valence manganites. *Adv. Phys.* **1999**, *48*, 167–293.

(2) Cava, R.; Batlogg, B.; Krajewski, J.; Farrow, R.; Rupp Jr, L.; White, A.; Short, K.; Peck, W.; Kometani, T. Superconductivity near 30 K without copper: the $Ba_{0.6}K_{0.4}BiO_3$ perovskite. *Nature* **1988**, *332*, 814.

(3) Zhao, D.; Wang, C.; Song, Z.; Yu, Y.; Chen, C.; Zhao, X.; Zhu, K.; Yan, Y. Four-terminal all-perovskite tandem solar cells achieving power conversion efficiencies exceeding 23%. *ACS Energy Lett.* **2018**, *3*, 305–306.

(4) Maughan, A. E.; Ganose, A. M.; Bordelon, M. M.; Miller, E. M.; Scanlon, D. O.; Neilson, J. R. Defect tolerance to intolerance in the vacancy-ordered double perovskite semiconductors Cs_2SnI_6 and Cs_2TeI_6. *J. Am. Chem. Soc.* **2016**, *138*, 8453–8464.

(5) Prassides, K.; Day, P.; Cheetham, A. K. Anion ordering in mixed valence dicesium hexachloroantimonate (Cs_2SbCl_6) and related salts. *J. Am. Chem. Soc.* **1983**, *105*, 3366–3368.

(6) Maughan, A. E.; Ganose, A. M.; Scanlon, D. O.; Neilson, J. R. Perspectives and Design Principles of Vacancy-Ordered Double Perovskite Halide Semiconductors. *Chem. Mater.* **2019**,

(7) Prassides, K.; Day, P.; Cheetham, A. K. Crystal structures of mixed-valency and mixed-metal salts $A_2M^{III}_{0.5}Sb^{V}_{0.5}X_6$ (A= Rb, Cs; M= Sb, Bi, In, Tl, Fe, Rh; X= Cl, Br). A powder neutron diffraction study. *Inorg. Chem.* **1985**, *24*, 545–552.

(8) Day, P. *Molecules Into Materials: Case Studies in Materials Chemistry—Mixed Valency, Magnetism and Superconductivity*; World Scientific, 2007; pp 120–124.

(9) Atkinson, L.; Day, P. Charge transfer in mixed-valence solids. Part IV. Electronic spectra of hexachloroantimonates (III, V). *J. Chem. Soc.* **1969**, 2423–2431.

(10) Clark, H.; Swanson, B. I. Effects of outer-sphere electron transfer on the vibrational spectrum of dicesium antimony hexachloride. *J. Am. Chem. Soc.* **1981**, *103*, 2928–2933.

(11) Toby, B. H. EXPGUI, a graphical user interface for GSAS. *J. Appl. Crystallogr.* **2001**, *34*, 210–213.

(12) Sheldrick, G. M. A short history of SHELX. *Acta Crystallogr. A.* **2008**, *64*, 112–122.

(13) Bruker, S. Version 6.02 (includes XPREP and SADABS). *Bruker AXS Inc., Madison, Wisconsin, USA* **1999**,

(14) Momma, K.; Izumi, F. VESTA: a three-dimensional visualization system for electronic and structural analysis. *J. Appl. Crystallogr.* **2008**, *41*, 653–658.

(15) Tilley, R. J. *Perovskites: structure-property relationships*; John Wiley & Sons, 2016.

(16) Fabini, D. H.; Laurita, G.; Bechtel, J. S.; Stoumpos, C. C.; Evans, H. A.; Kontos, A. G.; Raptis, Y. S.; Falaras, P.; Van der Ven, A.; Kanatzidis, M. G.; Seshadri, R. Dynamic Stereochemical Activity of the Sn^{2+} Lone Pair in Perovskite $CsSnBr_3$. *J. Am. Chem. Soc.* **2016**, *138*, 11820–11832.

(17) Brown, I. D. *Bond Valences*; Springer, 2013; pp 11–58.

(18) Howard, C. J.; Kennedy, B. J.; Woodward, P. M. Ordered double perovskites–a group-theoretical analysis. *Acta Crystallogr. B.* **2003**, *59*, 463–471.

(19) Niggli, P. XII. Die Kristallstruktur einiger Oxyde I. *Z. Kristallogr. Cryst. Mater.* **1922**, *57*, 253–299.

For Table of Contents Use Only

Hydrothermal Crystal Growth of Mixed Valence Cs_2SbBr_6

Victoria E. Combs, Iain W. H. Oswald, James R. Neilson

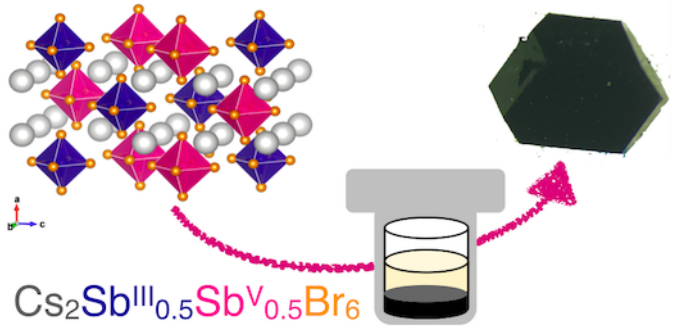

Synopsis

The preparation of high-quality single crystals of the mixed valence compound Cs_2SbBr_6 via hydrothermal synthesis is reported. Single crystal X-ray diffraction in conjunction with heat capacity measurements suggest an absence of any phase transitions between $T = 2$ to 380 K. Laue diffraction shows that Cs_2SbBr_6 crystals form large faces along the (001) and (112) planes.